International Journal of Engineering

Journal Homepage: www.ije.ir

Experimental and Numerical Study of Perforated Steel Plate Shear Panels

H. Monsef Ahmadi*[a], M. R. Sheidaii[a], S. Tariverdilo[a], A. Formisano[b], G. De Matteis[c]

[a] *Civil Engineering Department, Urmia University, Urmia, Iran*

[b] *Department of Structures for Engineering and Architecture, School of Polytechnic and Basic Sciences, University of Naples "Federico II", Naples, Italy*

[c] *Department of Architecture and Industrial Design University of Campania "Luigi Vanvitelli", Aversa, Italy*

PAPER INFO

Paper history:
Received 24 December 2019
Received in revised form 29 February 2020
Accepted 07 March 2020

Keywords:
Shear Panels
Perforated Pattern
Fracture
Shear Strength
Hysteretic Behavior
Finite Element Analysis

ABSTRACT

Thin perforated Steel Plate Shear (SPS) Walls are among the most common types of energy dissipating systems. The applied holes reduce the shear strength of the plate and allow to decrease the profile size of the members at the boundary of the panel when these systems are used in the typical design of structures. On the other hand, the different fracture locations of these panels are visible when considering the different perforation patterns. This paper reports on the results obtained from the experimental study under cyclic loading of the effect of different hole patterns on the seismic response of the systems and the location of the fracture. According to this, two perforated specimens by different patterns were considered. In addition, a plate without holes for a better comparison of the fracture location was chosen. The results showed that changing the pattern of the holes causes a change in the fracture location. Moreover, in perforated specimens, the amount of shear strength did not reduce suddenly after the fracture phenomenon. In the specimen which was perforated around the web plate, the pinching force was more than any other in the low cycle of the drifts. For this reason, the energy dissipation and initial stiffness were more than up to 3% drift. The experimental specimens were then simulated with a Finite Element (FE) method using the ABAQUS. Finally, a parametric FE analysis on different series of perforated panels, by changing the diameter of the holes and the plate thickness, has been carried out.

***doi**: 10.5829/ije.2020.33.04a.02*

1. INTRODUCTION

Steel Plate Shear (SPS) Walls are one of the seismic protection systems used to resist lateral forces in new and existing buildings. SPS walls have a low erection cost and quick installation time; they are usually obtained by inserting a metallic panel, which represents the main lateral load-resisting element inside a frame composed of steel beams and columns [1]. In SPS walls, energy dissipation takes place mainly due to a shear mechanism, through either pure shear stress or tension field action. A pure shear dissipative mechanism would be preferable, and it allows to have both a stable inelastic cyclic behavior as well as a uniform yielding spread over the entire panel. In order to have a pure shear dissipative mechanism, shear panels have to be designed and stiffened in such a way that to avoid any buckling phenomenon up to the required plastic deformation level [2]. This type of SPS walls can be defined as "compact," meaning that they did not suffer buckling phenomena upon reaching the required plastic deformation. On the other hand, when the plate thickness is very small, shear instability occurs due to the reduced value of the shear load and, consequently, the shear strength of the panel is governed by the tension field mechanism only, which is known as "slender" shear panels. The main advantages of using unstiffened shear panels are enhanced strength, stiffness and ductility, stable hysteretic characteristics, and a large capacity for plastic energy absorption. The buckling of the plate made of slender panels is not

*Corresponding Author Email: *Hadimonsefahmadi@gmail.com*
(H. Monsef Ahmadi)

Please cite this article as: H. Monsef Ahmadi, M. Sheidaii, S. Tariverdilo, A. Formisano, G. De Matteis, Experimental and Numerical Study of Perforated Steel Plate Shear Panels, International Journal of Engineering (IJE), IJE TRANSACTIONS A: Basics Vol. 33, No. 4, (April 2020) 520-529

synonymous with failure. The post-buckling strength of thin SPS walls, which can be several times its elastic buckling resistance, can provide substantial strength, stiffness, and ductility, as demonstrated for plate girder webs [3]. In order to reduce the shear strength of slender shear panels, allowing to easily obtain the capacity design criteria, which in turn reduces the demand on the main bearing frame, a solution based on the use of holes has been proposed [4]. Perforated SPS walls with a single [5] or multiple circular holes [6] have been recommended. Roberts and Sabouri-Ghomi [7], performed a series of sixteen quasi-static cyclic loading tests on unstiffened SPS walls with centrally placed circular openings of varying diameters. All the panels exhibited adequate ductility for the first four loading cycles without any significant loss in the load-carrying capacity. It was observed that the stiffness and ultimate strength of the panels reduced linearly with the increase in the diameter of the circular openings. Therefore, it was suggested that the strength and the stiffness of perforated SPS walls can be approximated conservatively by applying a reduction factor of (1-D/d) where (D is the perforation diameter and d is the height of the panel) to the strength and the stiffness of a similar un-perforated plate [7]. Berman and Bruneau [8] conducted experiments to investigate the efficiency of SPS walls with circular openings. The authors proposed an effective reduction factor to account for the reduced stiffness and strength of panels with multiple circular holes. After considering several options for the hole diameter and spacings, the final design of the infill panel had 20 circular openings staggered to be aligned diagonally at 45^{o}, with a diameter of 200 mm and horizontal/vertical spacing of 300 mm. The specimen displayed stable S-shaped hysteresis loops with little pinching. The observed elastic stiffness was 115 kN/mm. Yielding was first observed at a drift of 0.3%. The test was finally stopped at 3% drift when a column continuity plate fractured. Although the web panel did not fracture at this drift, severe damage, and distortions to the panel made it impractical to continue testing [8].

Moghimi and Driver [9] investigated the influence of perforations on SPS walls by comparing them with similar SPS wall systems with no perforations in their infill plates. All the openings were regularly spaced vertically and horizontally (at a distance of 280 mm) over the entire area of the infill plates. According to the perforation patterns, it was predicted that the shear resistance of the perforated SPS wall should be 0.6 times that of a solid wall. The pushover analysis showed that a reduction factor of 0.6 was a conservative evaluation [9]. Valizadeh et al. [5] experimentally investigated eight SPS panels with and without a circular hole and a scale of 1:6. In the unperforated panel, a fracture was observed on the locality of the panel-frame connection. In the perforated panels with a central hole, the fracture was observed around the holes with a smaller diameter and higher slenderness. The ductility was greater in the perforated specimens with a larger diameter.

In 2015, a numerical study was conducted by Wang et al. [10] on different types of perforated, unperforated, slotted, and stiffened SPS panels. The equivalent plastic strain (PEEQ) was used in finite element (FE) analysis to predict the place of fracture tendency. A comparison of the highest PEEQ with experimental specimens showed that the fracture location of the experimental specimens was accurately specified. In addition, the highest PEEQ distributed across the boundary elements in unperforated shear panels was compared to other specimens. Therefore, the perforated specimen had the lowest PEEQ in relation to the other specimens in the boundary elements. De Matteis et al. [4] carried out an experimental and numerical study on two SPS panels with a rectangular perforation pattern and nine circular holes with different diameters. In both specimens, a pinching phenomenon was observed in their hysteretic curve. In these specimens, severe damage was inflicted with increasing lateral displacement due to the increased rotation of the primary stresses between the holes. A comprehensive numerical study was then conducted on different types of steel and aluminum shear walls with different patterns of circular holes by Formisano et al. [11]. The comparison with existing experimental results showed how the highest Von Mises stress in the FE analysis was observed where the fracture occurred in the tested specimens. Due to a suitable hole pattern, the specimen with the opening ratio of 38% had a higher shear strength than the specimens with the opening ratios of 25 and 28%.

The failure mechanism of the butterfly [12] and honeycomb [13] shaped links of steel plate fuses has been evaluated by the PEEQ distribution. Based on this, when the PEEQ was uniformly distributed over the honeycomb-shaped links dampers, the failure mechanism has changed from beam flexural yielding to global plate buckling.

In this paper, experimental and numerical studies are investigated on three slender SPS panels - one unperforated and two perforated specimens. The perforated SPS walls are perforated in two ways; one of them is configured according to ANSI/AISC 341-16 [14]; while, the other is prepared according to the authors' opinion. Mainly, the present research aims to achieve the following goals:

- to investigate the hysteretic behavior of very thin perforated and unperforated shear panels through experimental tests;
- to suggest the novel perforation pattern;
- to evaluate the fracture tendency of the pecimens through FE analysis;

2. THE EXPERIMENTAL ACTIVITIES

A series of experiments were carried out on thin SPS panels at Structural Engineering Research Center (Urmia University) to investigate the cyclic behavior of SPS panels.

2. 1. Specimen Preparation The details of the tests are reported below. The three tested SPS panels that henceforth will be referred to as SP1, SP2, and SP3 were made of 0.7 mm thick plates. The diameter of the holes in each perforated specimen is 92mm (Figure 1).

A frame was used to investigate the behavior of SPS panels (as shown in Figure 2). The boundary members of the frame were made of an I-section IPE200 profile. The beam and column joints were made of 15-mm-thick sheets and were connected by M30 bolts with 8.8 grade. To allow for the easy connection of the metal sheet to the frame, a row of 16 M12-8.8 bolts were used at 50 mm intervals in 900 mm long fishplates of a 50 × 50 × 5 mm cross-section. The fishplates were completely welded to the frame.

Since the hydraulic jack in the laboratory was fixed on site, a cantilever beam of 2000-mm length was used to transfer the force from the jack to the frame. The column was connected by six bolts to the hydraulic jack. As illustrated in Figure 3a, the right side of the frame was connected to a rigid support. The out-of-plane displacement of the load transfer column was controlled by a beam box section 80 × 80 × 3 mm, in which the column was connected to restrain the beam by two wheels on either side (Figure 3b). The load transfer column was connected to the frame by a 20-mm thick and 300 mm long sheet. The frame was prevented from any out-of-plane displacements through restraining with two U120 profiles on either side, 400 mm long. The U-channel beams were seam welded to the load transfer column on one side and were tangent to the frame flange on the other side to allow the frame to move in the vertical direction. The mechanical properties of the SPS panels were subjected to standard tensile testing [16] by three coupon samples determined at the Razi Metallurgy Center. The samples were also quantum-tested to specify their composition. The results showed how the tested sheet specimens were made of cold-formed steel with a yield stress of approximately 175 MPa. The results of uniaxial tests are presented in Table 1.

The SAC recommended loading protocol [15] was used to examine the cyclic behavior of the SPS walls (Figure 4). All the SPS panels were tested by displacement-controlled loading by up to a maximum drift of 9% at a fixed rate of 40 mm/min.

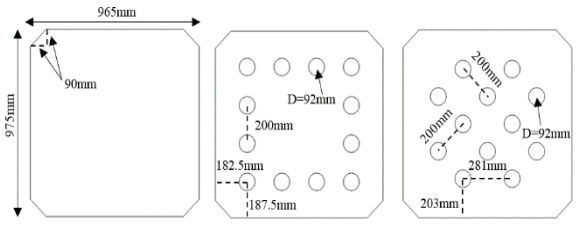

(a) (b) (c)

Figure 1. Plate details for experimented SPS walls: (a) SP1, (b) SP2 and (c) SP3

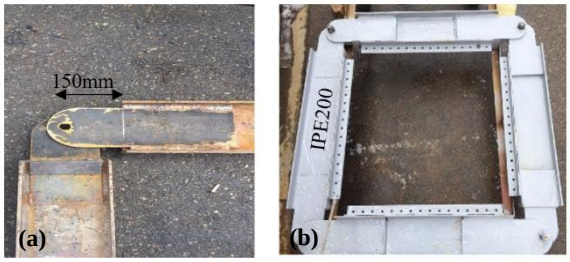

Figure 2. The frame setup: a) beam to column connection and b) the frame assembly

(a) (b)

Figure 3. Assembly the frame on jack and strong floor: a) The view of front b) out of plane restraint of jack

TABLE 1. Mechanical properties

Specimens	Modulus of elasticity (GPa)	Yielding stress (MPa)	Ultimate stress (MPa)
1	176.3587	173	306
2	176.9191	173	309
3	176.2125	177	307

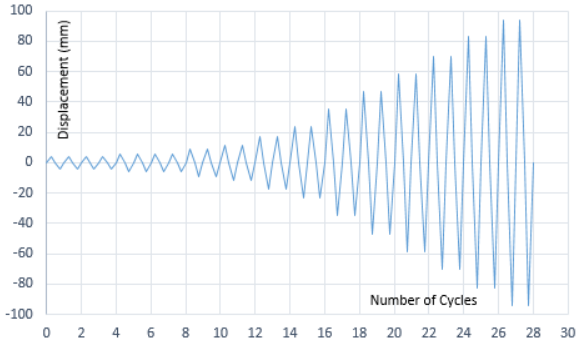

Figure 4. Loading protocol suggestion with SAC

2. 2. Test Observations of SP1 At the start of the experiment, the unperforated shear panel buckled significantly in the pressure and tensile directions, both normal to the plane. At 0.375% drift, the specimen was partially crushed at the bottom right corner. At 0.5% drift, the specimen buckled at the top left corner across half the length of the primary diameter. At 0.75% drift, the buckling of the previous step was extended, and the bottom left corner was partially crushed. At 1% drift, the noise made by out-of-plane deformations during the compression and tension of the specimen was considerably reduced compared to the previous steps (Figure 5a). At this level of drift, the tension field waves were increased near the panel-to-frame connection. Therefore, at a displacement = 0, the shear panel did not have a smooth surface and had pleats forming at the connection on the right that turned into a tension field by reaching the target displacement. At 2% drift, the tension field inclined were distributed across the panel with respect to the horizontal gradually developing throughout the entire web plate at 49°, and the panel becoming more pleated than the previous drift, thus featuring more out-of-plane deformation during unloading compared to the previous step. At 3 and 4% drift, tension field waves proliferate, and the out of plane deformation was relatively higher at this point. At 5% drift, a small fracture formed on the top right corner of the panel–frame connection. At 6% drift, the right corner of the shear panel fractured from the connection of the panel to the frame. Finally, at 7% drift, the experiment ended (Figure 6a).

2. 3. Test Observations of SP2 At the start of the test, the out-of-plane buckling was not significant in the case with the unperforated specimen. At 0.375% drift, the bottom right corner was slightly crushed, and in the final of this step, the top right corner of the panel was also crushed to some extent. At 0.5% drift, two small waves developed between the holes near the left bottom corner. At 0.75% drift, the waves increased but did not spread compared to the previous case. At 1% drift, the bottom left corner of the panel was slightly crushed, whereas the wrinkles were more severe in the tension field between the holes near the primary diameter (Figure 5b). At 2% drift, the tension field waves between the holes further away from the primary diameter were gradually mitigated. By this step, when reaching the target displacement = 23.5mm, the waves of the tension field intensified. At 3% drift, tension field waves developed at the connection of the panel to the frame but were much fewer than in the case of the unperforated specimen. At this point of the drift, the investigated out-of-plane buckling proved to be less than in the case with an unperforated specimen. It must also be noted that the specimen bent out of the plane along the primary diameter but sank under it. At 7% drift, the fracture was produced between the panel and frame connection in the right corner of the panel. At 8% drift, the four corners were slightly crushed, however, at 9% drift, the test ended with the fracture at the panel-to-frame connection extending without failure around the holes (Figure 6b).

2. 4. Test Observations of SP3 At the beginning, in the target displacement = 4.4 mm, buckling waves developed simultaneously in two directions, outward, above the primary diameter, and inward, in the bottom area. At 0.375% drift, the bottom right corner of the specimen, an outward-oriented buckling wave developed between the holes in the corners of the specimen and the corners of the panel, with an inward-oriented wave on the opposite side. By this step, the buckling was less significant than in the previous specimens. At 0.5% drift, the buckling waves were relatively more intense at the corners of the panel, with negligible tensile stresses developing around the holes. At 1% drift, as highlighted in Figure 5c, the tension field extended between the holes while being stable around the holes but not at the center of the panel. At 2% drift, the buckling waves were more severe between the holes and more stable concerning the previous case. However, at 3% drift, the waves were much more intense at the four corners of the panel. At 4% drift, the tension field inclination angle was measured to be 43° around the holes by this step. At 5% drift, as displacement increased in the four holes on the corners of the panel in relation to the other holes, they deformed from circular to oval-shaped holes. At 6% drift, the holes at the four corners of the panel were severely crushed. By this step of drift, the out-of-plane displacements of buckling were much less in the entire panel—in particular, at the center—than the previous specimens. At 7% drift, the panel-to-frame connection was much more stable than the previous specimens. However, the hole in the top right corner of the panel was fractured to some extent due to the severe crushing of the holes in all four corners at this displacement. At 8% drift, another fracture took place around the hole in the top left corner of the panel, but the fracture from the previous step extended to the center. At 9% drift, the intense buckling waves developed in the hole on the corner did not allow the crack to grow, and the test ended without failure at other holes (Figure 6c).

(a) **(b)** **(c)**

Figure 5. Deformed shape of 1% drift in a) SP1, b) SP2 and c) SP3

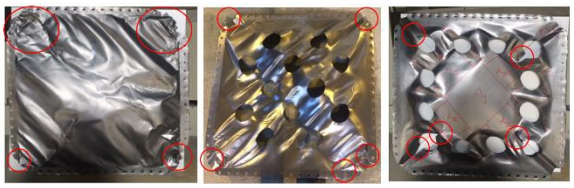

(a) (b) (c)

Figure 6. Fracture phenomenon at the end of processes of a) SP1, b) SP2 and c) SP3

3. TEST RESULTS

In this section, the hysteretic performance of the tested specimen was assessed based on the initial stiffness, shear strength, pinching force, and the energy absorption related to the obtained cyclic behavior (Figure 7). The load-displacement curves are shown in Figure 7 suggest that all the specimens have a pronounced pinching effect. The backbone curve was plotted for every hysteresis graph for comparison (Figure 8). As evident from Figure 8, the initial stiffness was higher with SP3 than the other two specimens in the positive region but lower than SP1 in the negative region. However, in SP1 and SP2, the initial stiffness in the positive region is not in line with that in the negative region, and there exists a sharp curvature that results in a lower stiffness than SP3 in the positive region.

3. 1. Fracture Evidence of SP1 At the first step of 6% drift, the maximum shear strength was 95.43 kN in the positive and negative regions. In the second cycle, at 6% drift, the shear strength is reduced by only 0.5%. In the first cycle of 7% drift, the shear strength was measured at 87 kN on average, while in the second cycle, it exhibited a 10% drop with fracture phenomenon.

3. 2. Fracture Evidence of SP2 At 7% drift, SP2 fractured with a maximum shear force of 74.85 kN before reaching the target displacement (82 mm), which reduced the shear strength in the positive range by 6.5%; however, the strength was measured similarly at 76.15 kN with no variation in the negative region. In the first cycle with 8% drift, the shear strength was at 74.85 kN in both the positive and negative directions. However, in the second cycle at 8% drift, the shear strength was 71.22 kN in the positive region and 65.85 kN in the negative region. In the first cycle with 9% drift, the shear strength was measured at 72.79 kN in the positive region and 75.72 kN in the negative region. However, in the second cycle at 9% drift, the shear strength was 64.59 kN in the positive region and 68.34 in the negative region.

3. 3. Fracture Evidence of SP3 At 7% drift, the maximum shear strength was measured at 66.75 kN in the positive range and 59.24 kN in the negative range. In the second cycle at 7% drift, the shear strength was reduced by 30% in both regions. In the first cycle with 8% drift, the maximum shear strengths in the positive and negative regions were 64.7 kN and 54.4 kN, respectively, while it was reduced by 8% in the second cycle. In the first cycle with 9% drift, the maximum shear strength was measured at 61.38 kN in the positive region and 48.81 kN in the negative region. In the second cycle, the shear strength was reduced by 20% in both regions.

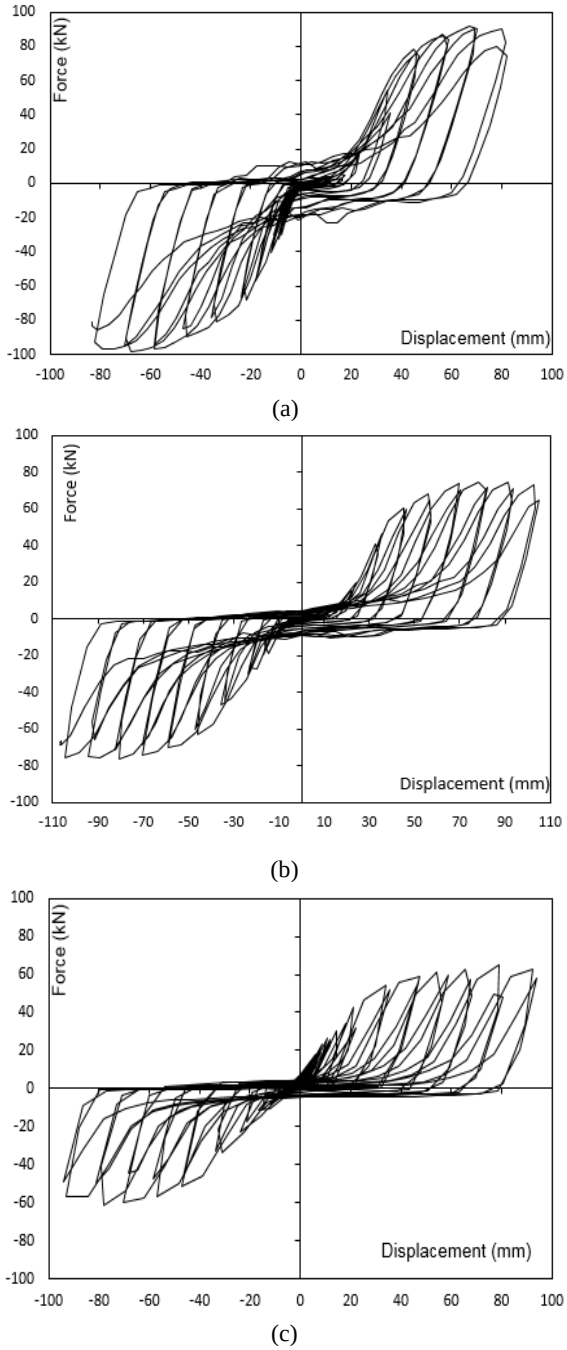

(a)

(b)

(c)

Figure 7. The hysteresis curves of a) SP1, b) SP2 and c) SP3

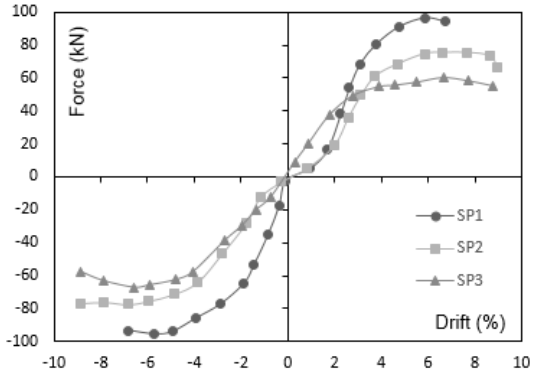

Figure 8. Comparison of backbone curves

3. 4. Summary of the Experimental Results The initial stiffness for the ideal bilinear curve for the laboratory specimens was prepared according to FEMA 356 [17] based on the equivalent energy, maximum shear strength, and ultimate shear strength of every specimen, which was obtained from the hysteretic curves presented in Table 2. Also, the cumulative energy dissipation was evaluated for each cycle of loading by summing the area under hysteretic curve created (Table 3).

As shown in Table 3, the cumulative energy dissipation of specimen without holes was significantly more than perforated SPS panels up to 3% drift. However, this value for SP3 was 30% more than SP2. At drifts 4 to 7%, the tension fields were distributed over the web plate in the SP1 and SP2; for this reason, the dissipated energy values were computed more than SP3 until 7% of drift. Furthermore, following the cyclic loading, the total dissipative energy of SP2 was higher than other specimens. It was expected because the test was stopped for the SP1 due to fracture phenomena at 7% of drift. Also, the tension fields were not distributed at the center of the SP3 after 7% of drift.

TABLE 2. Summary of experimental results

Specimens	Max strength (kN)		Ultimate strength (kN)		Initial stiffness (kN/mm)	
	F^{+}_{max}	F^{-}_{max}	U^{+}_{max}	U^{-}_{max}	K^{+}	K^{-}
SP1	95.4	94.37	86.66	79.47	0.44	3.5
SP2	74.8	76.15	72.8	75.7	0.53	1.1
SP3	66.7	59.24	61.4	48.8	2.6	1.43

TABLE 3. Results of cumulative energy dissipation

Specimens	up to 3% drift (kN.mm)	4 to 7% drift (kN.mm)	8 to 9% drift (kN.mm)
SP1	4418	32241	-
SP2	2297	20623	14480
SP3	2969	14221	6630

4. FINITE ELEMENT (FE) ANALYSIS

A Finite Element (FE) model was developed in ABAQUS [18] following the experimental models in order to study the behavior of SPS panels. Accordingly, the cyclic behavior of the three FE models was verified through experimental results.

4. 1. Description of Proposed FE Model B31 beam type elements were used to simulate the hinged frame with columns and beams center-to-center spacing of 975 mm and 965 mm, respectively. The connection of the primary elements of the frame was defined using the HINGE connectors. The plate was adopted by S4R shell elements. The TIE connectors were used for the surface-to-surface connection of the panel to the frame; besides, the fishplates had no impact on the results, they were ignored. The base advancing front mesh algorithm was adopted for the unperforated and perforated shear panels. An approximate mesh size of 50 mm was considered around the panel. Likewise, an approximate mesh size of 10 mm was chosen for around the holes (Figure 9). The fix boundary condition type was adopted on the frame supporting the connection place since it was completely welded. In the simulated model, the displacement of the transition beam elements and fishplate location elements in the shear panel was set perpendicular to the plate (Z-axis) with a rotation around the X- and Y-axis. The mechanical properties of the primary elements of the frame were similar to those of elastic steel materials.

Moreover, the combine hardening was selected for FE models on the yielding stress and plastic strains of the plate material based on the results from the tensile test (Table 1) in both the cyclic and pushover analyses. For a suitable simulation of the initial stiffness of the experimental specimens, an initial imperfection of 1mm was applied to the shear panel based on the first and second buckling modes. The acting load was similar to the experimental loading protocol, except that only one cycle was adopted in each loading stage to reduce the total number of cycles. All the specimens were studied using the general static analysis.

The results from the pushover and cyclic analyses of the FE model were compared to the experimental results (Figure 10). According to Figure 10, there is a good consistency between the FE analysis and the experimental results.

4. 2. Fracture Verification The maximum values of the equivalent plastic strain (PEEQ) in the simulated specimen were compared to the failure location of the experimental specimen to predict the

probable failure location [10]. The maximum values PEEQ exactly overlap with the critical areas in the shear panels in the FE models (Figure 11). However, in SP1 and SP2, the critical areas were located on the panel corners and panel-frame connection region. In SP3, the critical area was located around holes in the four corners of the panel. These areas were correctly predicted with the maximum values of PEEQ value by the FE model.

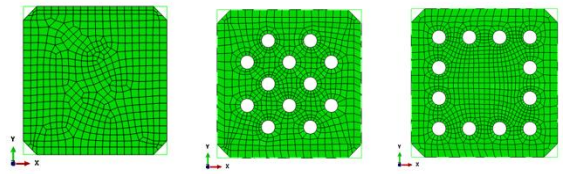

(a) (b) (c)

Figure 9. Suggested FE meshing: a) SP1, b) SP2 and c) SP3

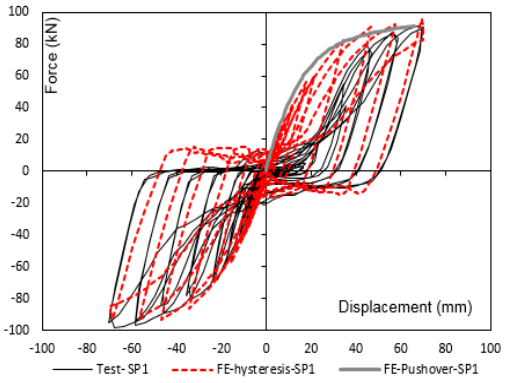

(a)

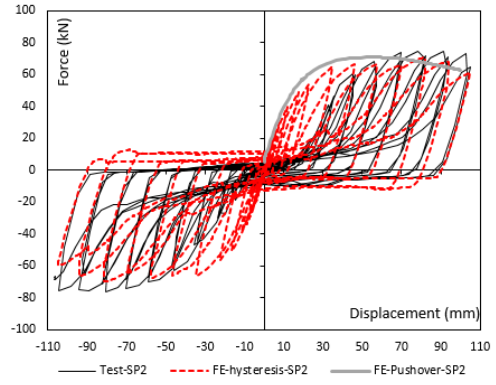

(b)

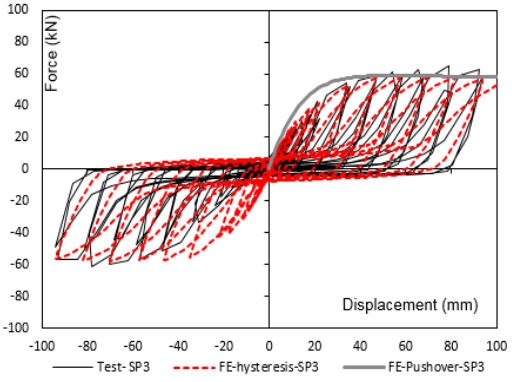

(c)

Figure 10. Verified experimental results with the FE model: a) SP1, b) SP2 and c) SP3

5. NONLINEAR PUSHOVER ANALYSIS ON SPS PANELS

Nonlinear FE analysis of a series of SPS panels was carried out using ABAQUS to determine the magnitude of the shear strength, yielding point, and initial stiffness. In total, three categories were considered in this section. Variation in perforation diameters (92 mm and 126 mm) and the web plate thickness (0.7 mm and 1.4 mm) were also considered for each type of perforation pattern.

5. 1. Pushover Analysis Model and analysis related to the perforation patterns of the two categories are shown in Figure 12. Furthermore, two solid plates (SP1) were analyzed as a reference in each category to compare the behavior with perforated SPS panels.

The perforated specimens were called SP2-D and SP3-D, which D is the perforation diameter in millimeters. The location of each hole in two perforated categories and also the material of the web plate were the same as the experimental one. A maximum target displacement of 100 mm was selected for all the pushover analyses. Pushover curves for all ten specimens are displayed in Figure 13.

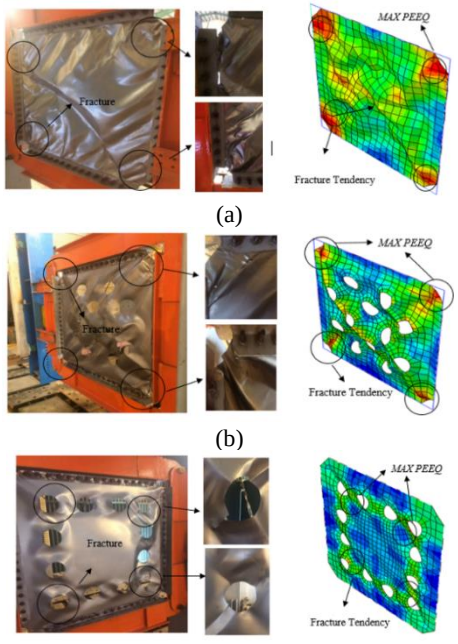

(a) (b) (c)

Figure 11. Equivalent the fracture tendency places with maximum PEEQ value in a) SP1, b) SP2 and c) SP3

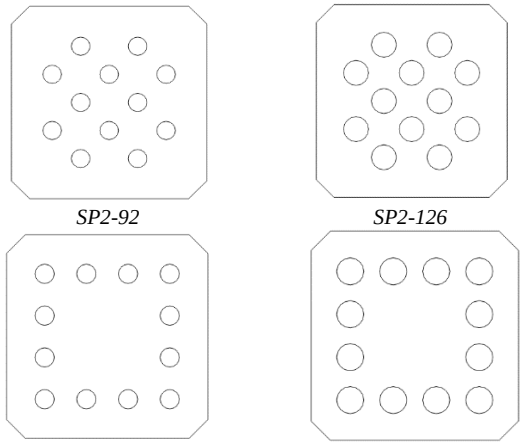

Figure 12. The perforated specimens categories for FE analysis

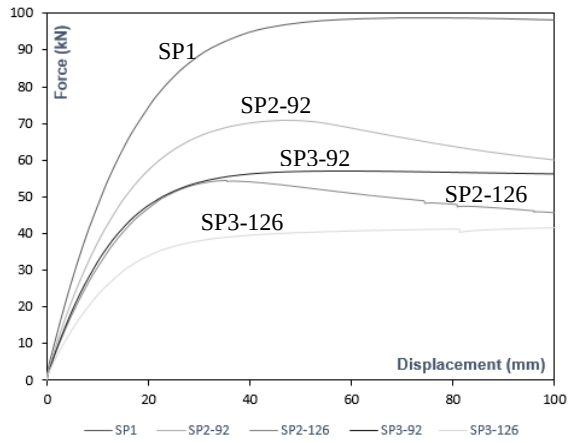

(a)

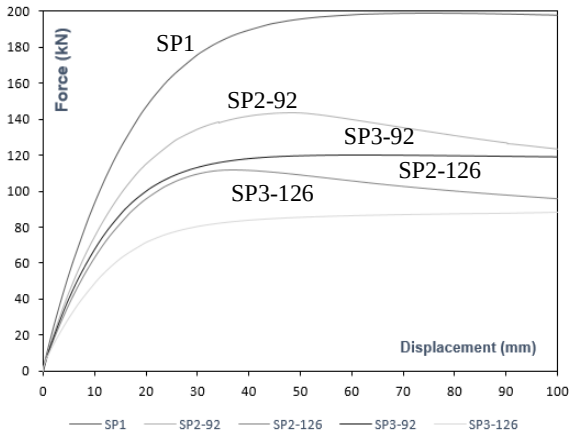

(b)

Figure 13. Pushover curves for SPS with thickness a) 0.7 mm and b) 1.4 mm

5. 2. Results and Discussion As shown in Figure 13, there is a growth in the shear strength and initial stiffness of SPS panels as the web plate thickness increases. The SP2 specimens have better performance in each perforation category, which was proved by the experimental test. Table 4 presents the maximum shear capacity, ultimate shear strength and, initial stiffness for all the specimens.

Since the specimens were made of two categories of perforation pattern, to have an easier comparison of the maximum shear strength and initial stiffness were normalized. Based on the FE results, shown in Table 4, the normalized ratio was obtained by dividing the maximum shear strength of perforated specimens (FP) over the maximum shear strength of the full panel (FF).

Likewise, normalization of the initial stiffness of specimens was obtained by dividing the initial stiffness of perforated specimens (KP) over the initial stiffness full panel (KF) (Figure 14).

The comparison between the normalized specimens SP2 and SP3 in Figure 14, indicated that the shear strength and initial stiffness could be controlled by changing the perforation pattern and diameter of holes. However, the shear strength and initial stiffness of the SP3-126 were decreased more than other specimens, which was expected, because increasing the diameter of holes, especially in the SP3 perforation pattern leads to decreasing the width between the holes. In this case, the global behavior of the web plate is constrained to the performance of behavior between holes.

6. EVALUATION OF SHEAR CAPACITY CALCULATING FORMULA

According to the material mechanics, the theoretical calculation formula for the shear capacity of solid plates (V_F), regular perforated plates (V_{p1}) and other perforation patterns (V_{p2}) which leave cut outed by circular holes of SPS walls are as Equations (1), (2) and (3) [19]:

$$V_F = 0.5F_y tL\sin(2\alpha) \quad (1)$$

$$V_{p1} = V_F(1-0.7\frac{D}{S_{diag}}) \quad (2)$$

$$V_{p2} = (L-N_r\beta\frac{D}{\cos\alpha})0.5F_y t\sin(2\alpha) \quad (3)$$

where: F_y is the yield stress, L is the clear distance between column flanges, α is the tension field angle , D is the circular hole diameter, S_{diag} is the diagonal distance between two consecutive perforation lines, N_r is the maximum number of diagonal strips with circular perforation, β is a regression constant (can be assumed 0.7 what was suggested in literature [19]), and t is the thickness of steel plate.

The yield strength of SP1 and SP2 category was calculated by Equations (1) and (2), respectively. Likewise, the yield strength of SP3 was obtained from

Equation (3). The N_r value was considered four because, as shown in Figure 11c, a significant portion of the center of the plate was not affected (no yielding); thus can be discounted.

As shown in Table 5, the yield strength of experimental specimens has been governed by prediction equations with minimum error.

TABLE 4. Summary of pushover results

Specimens	Max strength (kN)		Ultimate strength (kN)		Initial stiffness (kN /mm)	
Thickness (mm)	**t=0.7**	**t=1.4**	**t=0.7**	**t=1.4**	**t=0.7**	**t=1.4**
SP1	99	198	98	197	3.94	7.7
SP2-92	70	143	60	123	3.2	6.7
SP2-126	54	112	45	96	2.7	5.7
SP3-92	57	120	56	119	2.65	5.9
SP3-126	42	88	41	88	1.85	4.4

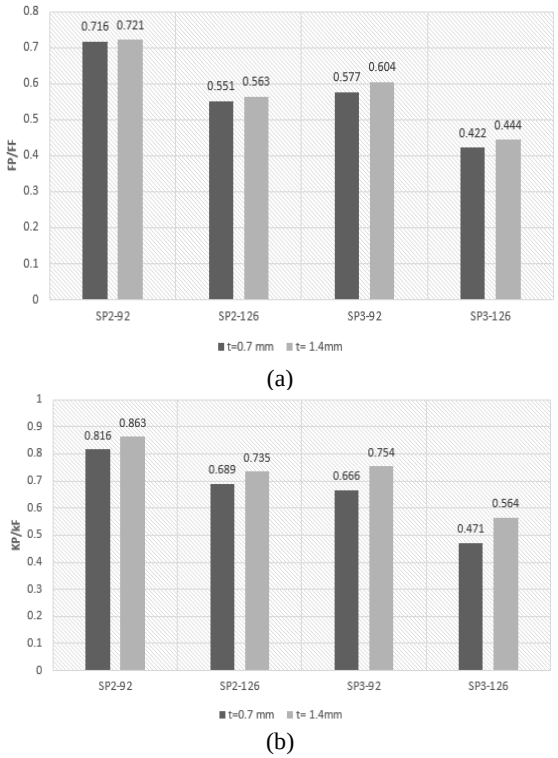

Figure 14. Comparison of normalized a) shear force and b) initial stiffness

TABLE 5. Yield strength results

Specimens	Experimental (kN)		Numerical (kN)		Theoretical (kN)	
Thickness	**t=0.7**	**t=1.4**	**t=0.7**	**t=1.4**	**t=0.7**	**t=1.4**
SP1	62	-	67	140	60	120
SP2-92	43	-	45	94	45	94
SP2-126	-	-	38	80	38	79
SP3-92	40	-	42	88	38	75
SP3-126	-	-	30	57	30	57

7. CONCLUSIONS

The present study was carried out to investigate through experimental tests the hysteretic behavior of three (two perforated and one unperforated) rolled Steel Plate Shear (SPS) panels under cyclic loading. One of the panels had an ANSI/AISC 341-16 perforation pattern. Investigating the failure location in the specimens SP1 and SP2 showed that fracture occurred at the panel-to-frame connection site at drifts 5 and 7%, respectively; while in the specimen SP3, the fracture occurred around four corner holes at drift 7%. After examining the hysteresis curves of the tested samples, the following results were obtained:

The specimens SP1 and SP2 in the positive area of the hysteretic curve have a lower initial stiffness than the specimen SP3. The initial stiffness of the SP3 in both the positive and negative areas of the hysteretic curve was greater than SP2. In the negative area of the hysteretic curve, the initial stiffness of the SP1 was greater than that of the two other perforated specimens. The maximum shear strength in the SP1 was equal to 95.43 kN at drift 6%, which decreased by 10% after fracture formation. In the perforated specimens, the maximum shear strength was equal to 75 kN in the SP2 and at drift 7%, which did not decrease after fracture formation at drift 8%, but decreased by 3% at drift 9%. The maximum shear strength in SP3 was equal to 66.75 kN at drift 7%, which decreased by 3 and 9% after fracture formation in drifts 8 and 9%, respectively. Due to the pinching effect of all the specimens and considering that the pinching force effects on the energy absorbed, the amount of energy dissipation was calculated. The SP3, up to drift 3%, has the highest pinching force compared to specimen SP2. For this reason, the energy absorption of SP3 increases. In drifts higher than 4%, the energy absorption grows by distributing the tension fields over the web plate for SP1 and SP2 specimens.

Based on the experimental results, a numerical model was simulated in the ABAQUS software. By comparing the maximum PEEQ value in the Finite Element (FE) method with the fracture location of the tested specimens, it was observed that the fracture location with this value was correctly predicted. Subsequently, FE analysis was implemented on two different perforation pattern categories. The results showed that the shear strength and initial stiffness of web plates could be controlled by changing the diameter of holes. On the other hand, increasing the diameter of holes, especially in the SP3

perforation pattern, leads to decrease in the width between the holes. In this case, the global behavior of the web plate was constrained to the performance of behavior between holes.

Finally, the yield strength of experimental and numerical analysis was governed by theoretical equations.

8. REFERENCES

1. Liu, J. and Astaneh-Asl, A., "Cyclic testing of simple connections including effects of slab", ***Journal of Structural Engineering***, Vol. 126, No. 1, (2000), 32-39.
2. De Matteis, G., Brando, G. and Mazzolani, F.M., "Pure aluminium: An innovative material for structural applications in seismic engineering", ***Construction and Building Materials***, Vol. 26, No. 1, (2012), 677-686.
3. Load, A., "Resistance factor design specification for structural steel buildings", American Institute of Steel Construction: Chicago, IL, USA, (1999).
4. De Matteis, G., Sarracco, G. and Brando, G., "Experimental tests and optimization rules for steel perforated shear panels", ***Journal of Constructional Steel Research***, Vol. 123, (2016), 41-52.
5. Valizadeh, H., Sheidaii, M. and Showkati, H., "Experimental investigation on cyclic behavior of perforated steel plate shear walls", ***Journal of Constructional Steel Research***, Vol. 70, (2012), 308-316.
6. Berman, J.W., Vian, D. and Bruneau, M., "Steel plate shear walls—from research to codification", in Structures Congress 2005: Metropolis and Beyond. (2005), 1-10.
7. Roberts, T.M. and Ghomi, S.S., "Hysteretic characteristics of unstiffened plate shear panels", ***Thin-Walled Structures***, Vol. 12, No. 2, (1991), 145-162.
8. Berman, J.W. and Bruneau, M., "Experimental investigation of light-gauge steel plate shear walls", ***Journal of Structural Engineering***, Vol. 131, No. 2, (2005), 259-267.
9. Moghimi, H. and Driver, R.G., "Effect of regular perforation patterns on steel plate shear wall column demands", in Structures Congress. (2011), 2917-2928.
10. Wang, M., Yang, W., Shi, Y. and Xu, J., "Seismic behaviors of steel plate shear wall structures with construction details and materials", ***Journal of Constructional Steel Research***, Vol. 107, (2015), 194-210.
11. Formisano, A., Lombardi, L. and Mazzolani, F., "Perforated metal shear panels as bracing devices of seismic-resistant structures", ***Journal of Constructional Steel Research***, Vol. 126, (2016), 37-49.
12. Farzampour, A., Khatibinia, M. and Mansouri, I., "Shape optimization of butterfly-shaped shear links using grey wolf algorithm", (2019).
13. Yang, T., Li, T., Tobber, L. and Pan, X., "Experimental and numerical study of honeycomb structural fuses", ***Engineering Structures***, Vol. 204, (2020), 109814.
14. ANSI, A., "341–16.(2016)", ***Seismic provisions for structural steel buildings***, 60601.
15. Venture, S.J., *Sac. Protocol for fabrication, inspection, testing and documentation of beam-column connection test and other experimental specimens. Sac rep*. 1997, SAC/BD-97/02, Sacramento, California.
16. Designation, A., "E8/e8m–09, standard test methods for tension testing of metallic materials", American association state highway and transportation officials standard AASHTO, T681-3.
17. Prestandard, F., "Commentary for the seismic rehabilitation of buildings (fema356)", Washington, DC: Federal Emergency Management Agency, Vol. 7, (2000).
18. ABAQUS, C., *Dassault systemes simulia*. 2018, Inc.
19. Bhowmick, A.K., Grondin, G.Y. and Driver, R.G., "Nonlinear seismic analysis of perforated steel plate shear walls", ***Journal of Constructional Steel Research***, Vol. 94, (2014), 103-113.

Persian Abstract

چکیده

دیوارهای برشی نازک از سیستم های رایج مستهلک کننده انرژی می باشند. ایجاد سوراخها در ورق اجازه کاهش اندازه اعضای مرزی دیوار برشی و کاهش مقاومت برشی ورق را که در طراحی متعارف سازه ها از این سیستم ها استفاده کرده اند را می دهد. از طرف دیگر، با درنظرگرفتن ارایش متفاوت سوراخ های پانل ها شکست های متفاوتی مشاهده می شود. این مقاله تاثیر آرایش متفاوت سوراخ ها بر رفتار لرزه ای و محل شکست این سیستم ها تحت بارگزاری چرخه ای بصورت آزمایشگاهی گزارش می دهد. بر این اساس، دو نمونه سوراخدار با آرایش متفاوت در نظر گرفته شده است. بعلاوه، یک ورق بدون سوراخ برای مقایسه بهتر محل شکست انتخاب شده بود. نتایج نشان داد که تغییر ارایش سوراخ ها سبب تغیر محل شکست می شود. علاوه بر این، در نمونه های سوراخ شده مقدار مقاومت برشی بعد از شکست بصورت ناگهانی کاهش پیدا نکرد. همچنین در نمونه ای که سوراخ ها در اطراف ورق قرار داشت مقدار نیروی پینچینگ در جابجایی های کوچک بیشتر از نمونه سوراخ شده دیگر بود. به این دلیل مقدار جذب انرژی و سختی اولیه آن نمونه تا سه درصد دریفت بیشتر بود. سپس ،نمونه های آزمایشگاهی توسط نرم افزار آباکوس با روش اجزا محدود شبیه سازی شده بودند. درنهایت، یک سری تحلیل اجزا محدود بر پانل های سوراخ شده، با تغییر قطرسوراخ ها وضخامت ورق انجام شده است.